

# Study of Unsaturated Polyester and Vinylester Morphologies Using Excimer Laser Surface Treatment

B. MORTAIGNE,<sup>1</sup> B. FELTZ,<sup>1</sup> P. LAURENS<sup>2</sup>

<sup>1</sup>DGA/DCE/Centre de Recherches et d'Etudes d'Arcueil, <sup>2</sup>LALP Unité mixte CREA/CNRS, 16 bis Avenue Prieur de la Côte d'Or, 94114 ARCUEIL cedex, France

Received 2 January 1997; accepted 3 May 1997

**ABSTRACT:** A technique based on the use of an ArF excimer laser (193 nm) to analyze the morphology of the unsaturated polyester and vinylester networks has been developed. This method is based on the use of the differences between the thresholds at which ablation of the various constituent phases of the materials occurs.

After having determined the ablation threshold of a polystyrene, various surface treatments using excimer lasers fluence around this threshold were applied to unsaturated polyesters and vinylester. In the latter case, a two-phase structure consisting of microgels in a polystyrene phase was shown by scanning electron microscopy observations, allowing us to conclude that the mechanisms by which vinylester and unsaturated polyester networks are formed are similar. We also observed that the two-phase structure of the vinylester matrixes, unlike that of the unsaturated polyesters, is organized rather than random-structured, which could represent a major parameter contributing to the very good hydrolysis stability of these materials. In the event of degradation by osmotic mechanisms, the organized structure network would enable limiting of the development of the osmotic pressures by distributing the forces within the material, thus avoiding crazing. © 1997 John Wiley & Sons, Inc. *J Appl Polym Sci* **66**: 1703–1714, 1997

**Key words:** unsaturated polyester; vinylester; microstructure; morphology; scanning electron microscopy; excimer laser; surface treatment; profilometry

## INTRODUCTION

Unsaturated polyesters (UP) are used in a large number of industrial applications for standard wear parts, but also for production of large-sized parts, such as ship hulls, owing to their relatively moderate cost with respect to the properties that they provide.<sup>1</sup> UPs provide good mechanical strength properties and are relatively easy to use. Associated with glass fibers, UPs can be implemented by contact techniques, such as by resin transfert molding (RTM). Associated with short fibers, UPs can be implemented by compression

techniques (SMC), injection techniques (BMC), and pultrusion.

The UPs consist of a prepolymer with ester functions in solution in a coreactant acting as a solvent and a crosslinking agent; the one used most often is styrene. Crosslinking takes place by radical polymerization mechanisms. The mechanisms by which thermosetting UP networks are formed have been studied by numerous authors. Horie et al.<sup>2,3</sup> performed differential scanning calorimetry (DSC) studies and were able to show that the crosslinking phenomena between the polyester chain unsaturations and between the styrene could not be explained solely on the basis of effects linked to the vitreous transition. Yang and Lee<sup>4,5</sup> studied the formation of thermoset networks by observing the rheology and the kinetics of systems during the process. Yang and Lee were

Correspondence to: B. Mortaigne

*Journal of Applied Polymer Science*, Vol. 66, 1703–1714 (1997)  
© 1997 John Wiley & Sons, Inc. CCC 0021-8995/97/091703-12

able to show that the UP network involved intermolecular reactions leading to the formation of a network, but it also intermolecular cyclization reactions. A microstructural study by Fourier transform infrared spectroscopy (FTIR) combined by microscopic observations<sup>6</sup> showed that the networks were formed by microgelling mechanisms with phase segregations. Microgels are intramolecularly crosslinked polymer particules that are stable when dispersed in a liquid phase and not soluble but, to some extent, swellable in the liquid phase. The particle size can be from 50 nm to a few microns. The particle size and the swellability can be controlled by the crosslinking density and the monomer composition of the liquid phase. In a theoretical work, Yang and Suspène<sup>7</sup> then Suspène et al.<sup>8</sup> put forward a model for the formation of microgels, which allowed them to foresee the evolutions in viscosity before the  $T_g$  during crosslinking. Kinetic and rheology studies showed that similar results could be obtained with UP networks modified by epoxy resins; IPN network;<sup>9</sup> or, in the case of modified networks, by low-profile additives.<sup>10</sup>

One of the major defects of the unsaturated polyester materials is their sensitivity to hydrolysis, which explains the large number of studies that have been carried out these past years on these materials, in particular to better understand the mechanisms by which blisters form on the surface of the materials used in the marine industry, both from a chemical point of view<sup>11</sup> and from a mechanical point of view.<sup>12,13</sup> One of the ways considered to explain the blistering produced by osmosis mechanisms<sup>14–16</sup> involves the formation of small soluble molecules that contribute to the development of an osmotic pressure and structural differences in the thermosetting UP network with different hydrophilicities, in which small hydrolyzed molecules could accumulate.

Unsaturated polyesters of a particular type, called vinyl esters (VE), and corresponding to a prepolymer chain (bisphenol A polycondensed with methylmetacrylate acid as cap end), have been developed to improve the hydrolysis stability of this class of materials. By limiting the chain ends in the UP networks and, therefore, the small hydrolyzable molecules (the major factor identified in degradation of these materials<sup>17</sup> by osmosis), the hydrolysis stability<sup>18,19</sup> is incontestably improved.

To better understand the formation of these VE networks, polymerization kinetic studies were performed.<sup>20</sup> If the results obtained by FTIR seem

to indicate that the VE network involves microgelling mechanisms similar to those observed for the UPs, with some phases rich in polystyrene and others rich in prepolymer, the microscopic observations carried out after preparation of the specimens by fracture in liquid nitrogen, then osmium coloration of the residual unsaturations<sup>21,22</sup> did not show the structural differences in the network formed by the microgels. Lasers are used to modify the surface characteristics of the materials to improve the properties in a large number of industrial applications (surface-activated for bonding, alloy deposits, etc.).<sup>23,24</sup> Numerous types of lasers have been developed and are commercially available. These devices cover a large energy range. For the surface treatments, the most commonly used lasers are CO<sub>2</sub> and Nd : YAG lasers in the infrared (IR) field and excimer lasers in the ultraviolet (UV) field. Excimer lasers are well adapted to the treatment of thermally sensitive materials, such as polymers. Due to the strong absorption of polymers in the UV range and the short duration of the laser pulse (few tens of nanoseconds), excimer lasers induce only very localized effects on the surface and prevent degradation of the bulk material (the modified layer thickness ranges between a few tenths of nanometers and a few micrometers). The nature of the physical phenomena taking place during the laser–surface interaction is strongly related to the laser fluence, i.e., the flux of incoming UV photons. When the fluence exceeds a threshold value (ablation threshold), material ejection from the surface occurs via photothermal and/or photochemical effects (ablation regime).<sup>25–27</sup> Surface ablation under UV laser radiation has found interesting applications such as surface cleaning, cornea surgery, micromachining (drilling and patterning), or thin film deposition. Below the ablation threshold (surface treatment regime), the laser irradiation is responsible for changes in the surface properties (chemical modifications, surface amorphisation); this can be used to improve the adhesive bonding properties of polymers or composite materials.<sup>28,29</sup> Ablation threshold and ablation rates are strongly dependent on the chemical composition of the polymer surface and on the laser wavelength.<sup>30–32</sup> This has to be related to the differences in the absorption coefficients of the polymers, the nature of the physical phenomena responsible for ablation (photochemical, photothermal, or both effects), and the chemical reactivity of the materials.

Within the frame of this work, our aim was to develop an analysis technique using the differ-



**Table I Code, Molar Compositions, and Physicochemical Characteristics of Unsaturated Polyester Under Study**

Code	Prepolymer Chemical Composition				Prepolymer Mass Ratio (1 s)	Styrene Mass Ratio (s)	$T_g$ (K)
	Maleate Molar Fraction	Isophthalate Molar Fraction	Propylene Molar Fraction	Neopentyl Molar Fraction			
A40	0.45	0.55	1	0	0.60	0.40	393
A45	0.45	0.55	1	0	0.55	0.45	390
A50	0.45	0.55	1	0	0.50	0.50	386
A55	0.45	0.55	1	0	0.45	0.55	380
B35	0.5	0.5	0.5	0.5	0.65	0.35	388
B38	0.5	0.5	0.5	0.5	0.62	0.38	389
B45	0.5	0.5	0.5	0.5	0.55	0.45	386
B50	0.5	0.5	0.5	0.5	0.50	0.50	385

The mean number molecular weight of the prepolymer, defined by steric exclusion chromatography, is 1000 daltons.

The detailed compositions of the vinyl ester materials used in this study, and the resin codes are given in Table II. As for unsaturated polyester networks, index on the sample references correspond to the weight fraction of styrene in the specimen.  $T_g$  are determined using the same conditions as for UP networks.

Before the experiment, the unsaturated polyester prepolymers A and B and the VE prepolymer were weighed and mixed with styrene monomer in a flask at the desired molar ratio (*s* percent weight). Each mixture was mixed for one hour at ambient temperature with a magnetic stirrer to dissolve the polyester prepolymer in the styrene monomer. Thus the samples studied differed by the weight fraction of styrene in the initial reactive mixture.

Plates 2 mm thick were molded from the resin mixtures. The cure was initiated at room temperature by a solution of cobalt octoate as catalyst

and by methyl-ethyl-ketone peroxide as promoter. The polymerization mechanism was of radical type. The concentration of catalyst and promoter was 0.3 and 1.2% by weight of total resin, respectively, for all samples (UP and VE). The samples were cured for 10 hours at 80°C, followed by 2 hours at 120°C.

Before the surface treatment by excimer laser, the surface of the samples (20 × 20 mm) was polished to obtain a roughness of less than 1 μm.

### Experimental Details

The laser treatment was performed using a pulsed ArF excimer laser ( $\lambda = 193$  nm; pulse duration = 16 ns), a Lamda Physics LPX 210 apparatus. The incident excimer laser beam was homogenized and shaped through an homogenizing device in order to obtain a square homogeneous irradiated area on the sample surface (the homogeneity for the fluence distribution was  $\pm 5\%$ ). Treatments were realized in air atmospheric pressure. The fluence of the incident laser beam ranged between 10 and 35 mJ/cm<sup>2</sup>. Modifications of the fluence was realized either by varying the laser voltage and/or by introducing attenuating optics in the beam path. The pulse repetition rate was 10 Hz, and the number of pulses was 200.

A Jeol scanning electron microscope, 6300F serie apparatus, with 12 kV power was used to view the surface polymer sample at magnifications from 1000 to 3000×. Before observation, the samples were dried at room temperature for 24 hours and platinum-coated for morphological measurement. Samples were observed with a 15° inclination. Ablation threshold and ablated depths were

**Table II Code, Molar Compositions, and Physicochemical Characteristics of Vinyl ester Under Study**

Code	Prepolymer Mass Ratio (1 s)	Styrene Mass Ratio (s)	$T_g$ (K)
VE40	0.60	0.40	380
VE45	0.55	0.45	383
VE50	0.50	0.50	378
VE55	0.45	0.55	375

**Table III Ablated Depths of PS, UP A, UP B, and VE for Different Fluences and Different Numbers of Pulses**

Laser Conditions		Ablated Depth (Å)			
Fluence	Number of Pulses	Polystyrene (PS)	Unsaturated Polyester A (UPA)	Unsaturated Polyester B (UPB)	Vinylester (VE)
15 mJ/cm <sup>2</sup>	200	<1000	0	0	0
	1000	<1000	0	0	0
20 mJ/cm <sup>2</sup>	200	1000–1500	0	0	0
	1000	2500–3000	0	0	0
25 mJ/cm <sup>2</sup>	200	3000–4000	<1000	<1000	<1000
	1000	15000	<1000	<1000	<1000
30 mJ/cm <sup>2</sup>	200	7000–8000	2000	1000	1500
	1000	20000–30000	3000–4000	2500–3000	2000–3000
10 mJ/cm <sup>2</sup>	1000	0	0	0	0

estimated by profilometry for the different materials, just after laser treatment and before SEM observation.

## RESULTS AND DISCUSSION

### Determination of Ablation Threshold

Before morphology analysis, PS, UP samples A and B, and the VE sample were laser treated at different fluences (10, 15, 20, 25, and 30 mJ cm<sup>-2</sup>) for 200 and 1000 pulses. Samples were then analyzed by profilometry to determine ablation threshold, and the results are reported in Table III.

For UP A and B and VE samples, the laser treatment at a fluence lower than 25 mJ/cm<sup>2</sup> did not induce ablation nor a change in the surface roughness; whereas, for fluences higher than 10 mJ/cm<sup>2</sup>, modifications were evidenced on PS samples.

Treatment at 15 mJ/cm<sup>2</sup> on PS samples and at 25 mJ/cm<sup>2</sup> on UP A, UP B, and VE samples induces changes mainly in the surface roughness, probably resulting from surface melting and/or slight surface ablation. Ablation depths (if ablation occurs in these conditions) could not be estimated by profilometry. When increasing the laser fluence (fluence > 15 mJ/cm<sup>2</sup> for PS samples and fluence > 25 mJ/cm<sup>2</sup> for UP and VE samples), surface ablation occurs, and ablated depths can be estimated. It can be seen that ablated depth increased with both the fluence and the number of pulses.

From the above results, it can be concluded that the ablation threshold fluence of PS is around 15

mJ/cm<sup>2</sup>, whereas UP and VE samples required higher fluence for ablation to occur. In the latter case, the ablation threshold is located around 25 mJ/cm<sup>2</sup>. No real and significant difference can be observed between UPA, UP B, and VE materials when increasing the fluence above the ablation threshold.

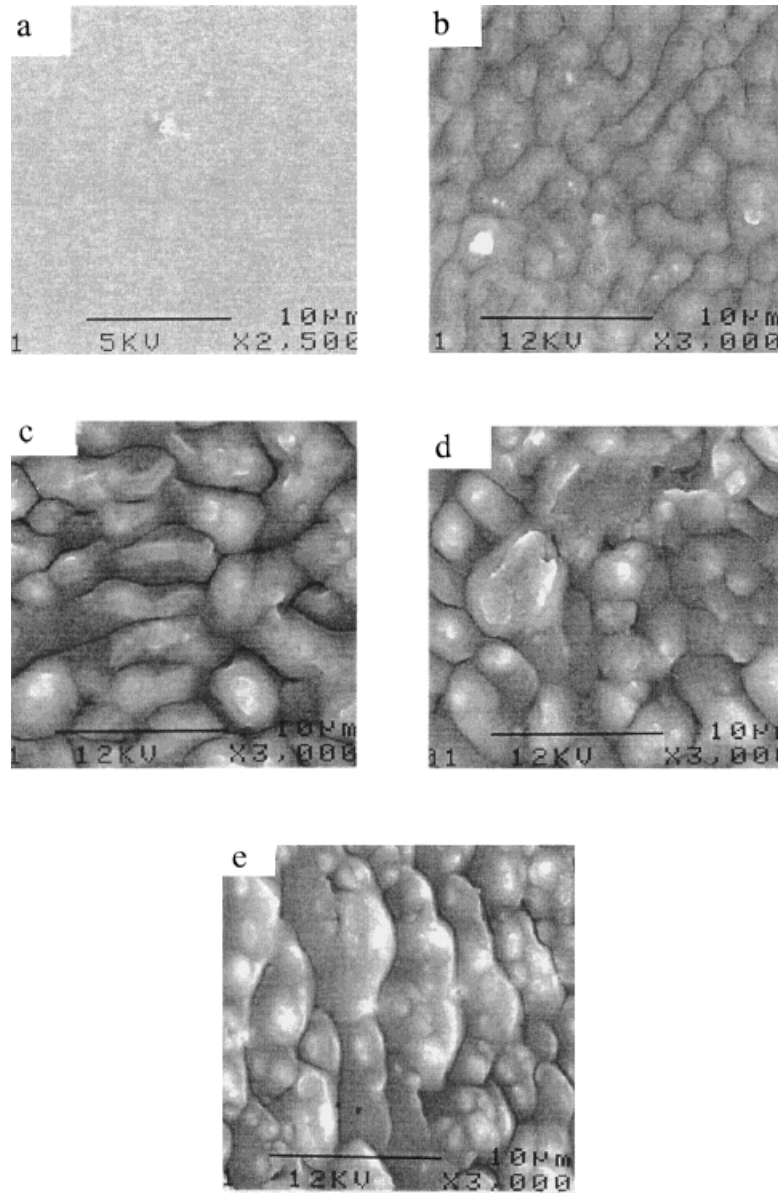
### PS Surface Analysis

Figure 1 represents the surface morphology of the PS after excimer laser treatment with fluence of 10, 15, 20, 25, and 35 mJ/cm<sup>2</sup>. Note for a surface morphology greater than 20 mJ cm<sup>-2</sup>, it seems that the samples melted on the surface and that a portion was ablated before the material could resolidify during the cooling phase after the laser pulse. With a heat capacity of 1.2 kJ<sup>-1</sup> kg K<sup>-1</sup> at 50°C (1.8 kJ<sup>-1</sup> kg K<sup>-1</sup> at 100°C) and a melting point of 240°C for polystyrene polymers,<sup>33</sup> the energy created by one pulse corresponds to the energy required to melt polystyrene in the volume of 1 cm<sup>2</sup> × 500 nm thick.

Starting with an energy of 20 mJ/cm<sup>2</sup>, and with 200 pulse shots, the surface temperature of the samples is greater than the polystyrene's melting point. The drops formed have a diameter of around 5 μm, and this occurs when the energy supplied is greater than the material's melting threshold. Beyond the 20 mJ cm<sup>-2</sup> threshold, the surface morphology after treatment is the same, with the surplus energy serving to ablate the melt phase.

### UP Sample A

With surface ablation of a polystyrene under excimer laser radiation (ArF) occurring at around 15



**Figure 1** SEM observation of polystyrene sample after ArF laser excimer treatment (193 nm radiation) with (a) 10, (b) 15, (c) 20, (d) 25, and (e) 35 mJ/cm<sup>2</sup>. Magnification is 3000 $\times$ .

mJ/cm<sup>2</sup>, we started by treating the surface of an unsaturated polyester type material crosslinked by radical mechanisms for which the two-phase structure of a polyester nodular network in a polystyrene phase is well established.<sup>4,7</sup>

Figure 2 represents the surface of the A45 samples after treatment by 200 pulse shots at 15, 20, 25, and 35 mJ/cm<sup>2</sup>. At 15 mJ/cm<sup>2</sup>, there is no change in the surface of the samples. For a treatment energy of 20 mJ/cm<sup>2</sup> [Fig. 2(b)] fluence above the ablation threshold for PS and below the ablation threshold for UP A, nodules begin to

appear on the surface of the samples. As calculated before, in this case, the energy applied to the surface of the samples is sufficiently high to melt and ablate the polystyrene phase. Not only are the nodules detected in materials implemented with very low styrene levels (35%), for which the polystyrene phase formed during the operation is minimal, but also in cases of tests where a much higher number of laser shots (up to 500) are performed to be sure to have eliminated all of the material which could be ablated. For these reasons, these nodules are attributed to

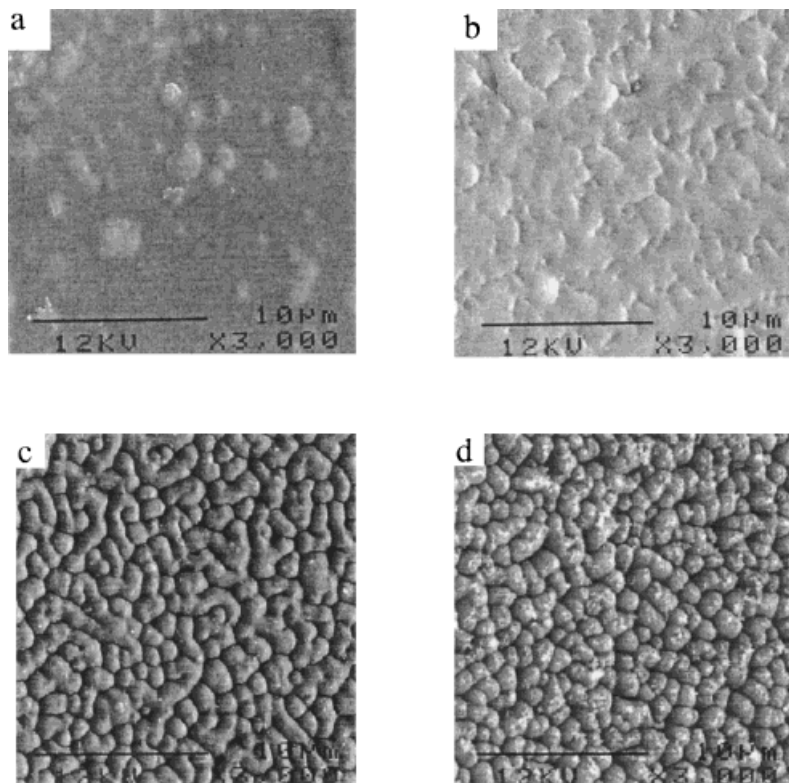


**Figure 2** SEM observation of unsaturated polyester G703 material with 45 wt % styrene (A45 sample) after ArF laser excimer treatment (193 nm radiation) with (a) 15, (b) 20, (c) 25, and (d) 35  $\text{mJ}/\text{cm}^2$ . Magnification is 3000 $\times$ .

polyester microgels. We can thus say that at 20  $\text{mJ}/\text{cm}^2$ , the polystyrene phase is attacked without attacking the polyester phase. At 25  $\text{mJ}/\text{cm}^2$  [Fig. 2(c)], fluence close to the ablation threshold of UP A, the entire polystyrene phase was melted and ablated with no major attack of the phase formed by the microgels of the unsaturated polyester network. The principle of microgel synthesis is to introduce crosslinking sites in micellar dimensions or, in other words, to form polymer networks within preorganized structures.<sup>34</sup> This ablation energy is in agreement with the previous experiments conducted on the PS. The polyester nodules are relatively long, 4 to 5  $\mu\text{m}$ , with a diameter of around 2  $\mu\text{m}$ . For an energy of 35  $\text{mJ}/\text{cm}^2$ , ablation of both PS and UP occurs, and cones appear with a feather structure at the peak, as classically occurs with surface treatment of polymers by excimer laser to improve adhesion characteristics.<sup>28,29</sup> For this treatment energy, the two phases (polyester and polystyrene) are attacked.

Figure 2 shows typical examples in which, at a suitable energy intensity, it was possible to ablate the polystyrene phase effectively without affect-

ing the UP phase. With the optimized processing parameters (200 shots, 25  $\text{mJ}/\text{cm}^2$ ), the excimer laser beam can selectively etch the constituent phase of the polymer matrix.

With samples A40, A50, and A55, the changes in morphology after surface treatment are identical to those observed for the A45 samples, meaning identical ablation thresholds. With this type of unsaturated polyester (type G703 thermoset network), it is thus possible to situate the threshold at which ablation of the polystyrene phase occurs, consisting of very short links forming a thermosetting material under ArF radiation at 15  $\text{mJ}/\text{cm}^2$ , the entire phase being ablated for an energy of 25  $\text{mJ}/\text{cm}^2$ .

#### UP Sample B

In this part of the work, we sought to verify whether the selective ablation determined for a type G703 unsaturated polyester was applicable to other unsaturated polyesters having different chemical structures.

Figure 3 shows the surface morphology of the

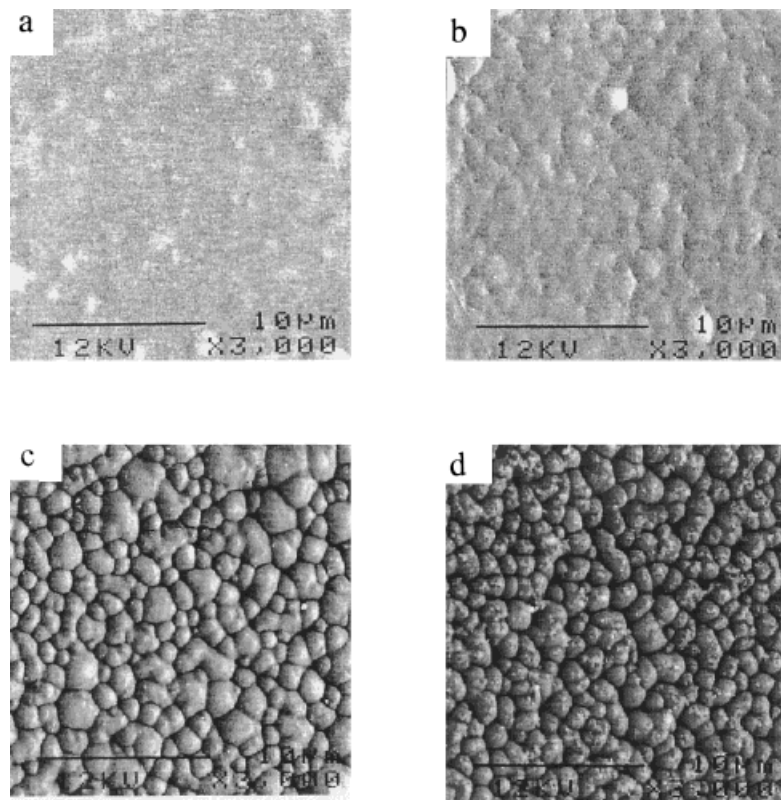


**Figure 3** SEM observation of unsaturated polyester G710 material with 35 wt % styrene (B35 sample) after ArF laser excimer treatment (193 nm radiation) with (a) 15, (b) 20, (c) 25, and (d) 35 mJ/cm<sup>2</sup>. Magnification is 3000 $\times$ .

B35 unsaturated polyester samples after treatment by an excimer laser. For a surface treatment energy intensity of 20 mJ/cm<sup>2</sup>, polyester nodules begin to appear in the polystyrene matrix in the same way as for the polyester samples of the A series. At 25 mJ/cm<sup>2</sup> [Fig. 3(c)], the entire polystyrene phase was ablated; and at 35 mJ/cm<sup>2</sup> [Fig. 3(d)], the two phases of the material were attacked. Two nodule sizes were identified, with some having a spherical shape with a diameter of around 2  $\mu$ m, and other smaller ones with a diameter of 1  $\mu$ m.

For samples B38, B45, and B50, as before, the nodules formed by the polyester phase were detected, starting at a surface treatment energy intensity of 20 mJ/cm<sup>2</sup>; and the polystyrene phase on the surface was removed at 25 mJ/cm<sup>2</sup>. However, on Figure 4, we have shown the surface of samples B38, B45, and B50 subjected to a radiation of 25 mJ/cm<sup>2</sup>. Here we observe that the size of the nodules decreases proportionally as the levels of styrene initially present in the original resin are lower. With the B38 samples, the nodules are

regular in size (spherical with diameter of 1.5  $\mu$ m); whereas in samples B45 and B50, the nodules formed are of different size. The structure of the B38 [Fig. 4(a)] network is very similar to that of the A45 network (Fig. 2). Drawing a parallel with the glass temperatures ( $T_g$ ) of the materials, we can see that these materials, in their series, show the highest  $T_g$ . This size and morphology of the nodules must be linked to the changes in viscosity during the gelling phase occurring during the treatment. The lower the styrene level, the faster the gel point is reached, with a low reaction lead. With the B50 sample [Fig. 4(c)], the nodules formed during microgelling can reach up to 4  $\mu$ m in diameter. These nodules have the time to grow before being totally immobilized with the empty spaces left between them filled in by smaller nodules, which would explain the morphologies observed.

As concerns the aging stability of these materials, the polyester networks obtained with an initial styrene percentage of 38% showed the best hydrolysis behavior.



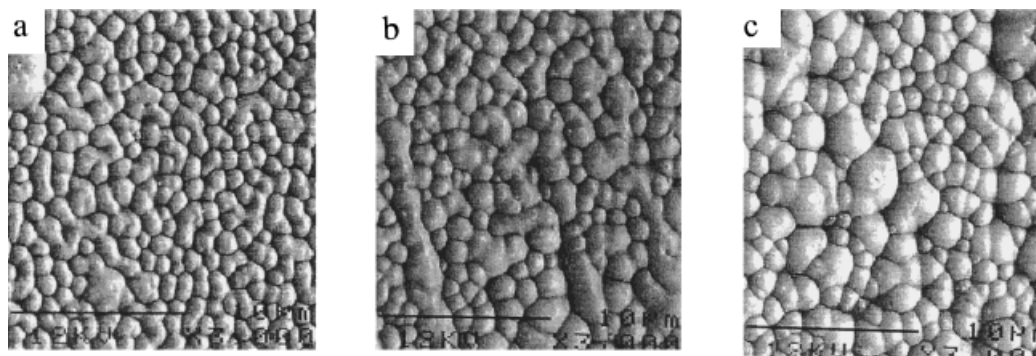


**Figure 4** SEM observation of unsaturated polyester G710 material with (a) 38 wt % styrene (B38 sample), (b) 45 wt % styrene (B45 sample), and (c) 50 wt % styrene (B50 sample) after ArF laser excimer treatment (193 nm radiation) with a  $25 \text{ mJ/cm}^2$  surface energy treatment. Magnification is  $3000\times$ .

### VE Sample

In this part of the work, we will use the selective laser ablation thresholds determined above to attempt to shed new light concerning the polymerization of the vinyl ester materials by microgelling mechanisms similar to those observed with unsaturated polyesters and to try to better understand the structure of these materials.

Figure 5 shows the surface of the samples of vinyl ester crosslinking agent whose resin contained 40, 45, 50, and 55% styrene during the operation, following exposure of the surface to an energy intensity by ArF excimer laser of 15, 20, 25, and  $35 \text{ mJ/cm}^2$  (200 shots).

In all the cases presented for an energy intensity of  $15 \text{ mJ/cm}^2$  [Fig. 5(a), (e), (i), and (m)], the surface of the samples was not ablated, though the surface of the samples seemed to be more modified than that of the UPs treated under the same conditions. At  $20 \text{ mJ/cm}^2$ , PS was ablated; and the nodules can be clearly seen in a way similar to those detected in the unsaturated polyesters treated at  $25 \text{ mJ/cm}^2$  [Figs. 2(c) and 3(c)]. For surface treatment energy intensities of 25 and  $35 \text{ mJ/cm}^2$ , both materials are ablated, and nodules with feather structures at their peak can be seen, meaning that the material has been attacked in its entirety.

For the VE50 samples, starting at  $15 \text{ mJ/cm}^2$ , the nodular structure of the material can be observed. At  $20 \text{ mJ/cm}^2$ , for the VE50 samples [Fig. 5(j)], the nodules are regular and similar to those of the UP samples (A45, B38); whereas for the VE samples (40 and 45), nodules of 1 and  $3 \mu\text{m}$  form the structure of the materials. With the VE50 samples, the size of the nodules observed is

smaller than that of the vinyl ester nodules of the VE40 and VE45 samples.

The PS phase formed being relatively high in this case, as shown in the previous studies using IR techniques,<sup>20</sup> the molar mass of the links is high, and the minimum energy intensity to be applied to ablate the phase is very close to that evaluated in the polystyrene surface treatment case.

With the VE45 samples, using a treatment of  $25 \text{ mJ/cm}^2$ , the network nodules are not yet attacked.

To give a comparison, Figure 6 shows the surface of the A45 and VE45 polyester samples magnified  $1000\times$ . With the unsaturated polyesters, the polyester nodules in the polystyrene are random oriented; whereas with the vinyl ester materials, the microgels seem to be organized. Though it is difficult to conceive an arrangement of the micronodules as they are forming during polymerization of this material, the fact that the material is structured could explain why, under microscopic analysis after osmium coloration of the residual styrene unsaturations, it was not possible to show the two-phase structure of the material (uniform distribution of the coloring agent on the surface of the material). Explanation of this arrangement could be done by considering physical polymerization, i.e., hydrogen bonding or coulomb interactions. Microgel particle synthesis using this principle is classically used to chemically crosslinked species as film material.<sup>34</sup> For example, it was proven that in the case of hydroxyacrylate, or methacrylate<sup>35</sup> crosslinked in the presence of a high quantity of hydroxyl group in the growing polymer chain (as polyester), leads to

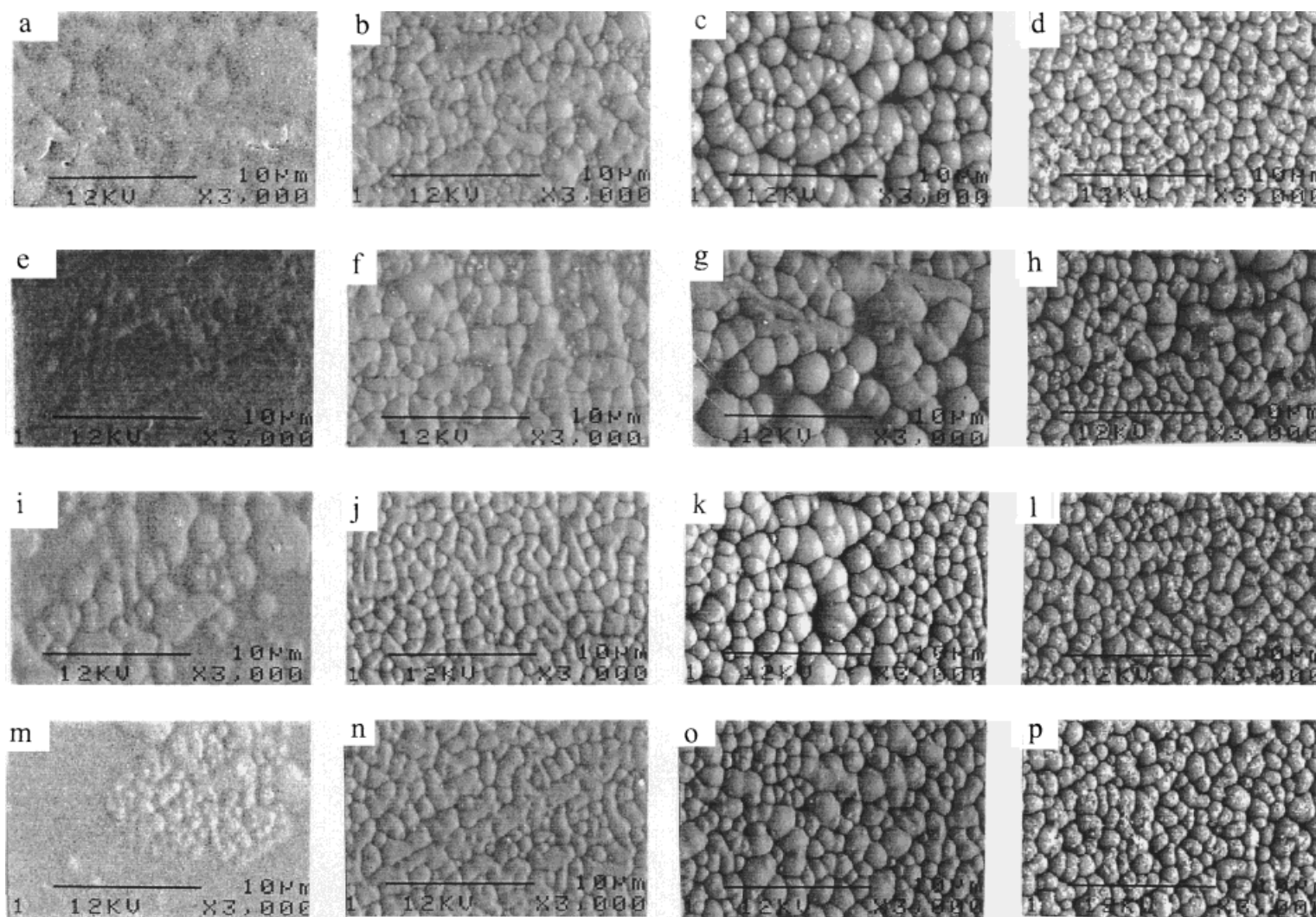


**Figure 5** SEM observation of vinylester material after ArF laser excimer treatment (193 nm radiation). Magnification is 3000 $\times$ : (a) VE40, 15 mJ/cm<sup>2</sup>; (b) VE40, 20 mJ/cm<sup>2</sup>; (c) VE40, 25 mJ/cm<sup>2</sup>; (d) VE40, 35 mJ/cm<sup>2</sup>; (e) VE45, 15 mJ/cm<sup>2</sup>; (f) VE45, 20 mJ/cm<sup>2</sup>; (g) VE45, 25 mJ/cm<sup>2</sup>; (h) VE45, 35 mJ/cm<sup>2</sup>; (i) VE50, 15 mJ/cm<sup>2</sup>; (j) VE50, 20 mJ/cm<sup>2</sup>; (k) VE50, 25 mJ/cm<sup>2</sup>; (l) VE50, 35 mJ/cm<sup>2</sup>; (m) VE55, 15 mJ/cm<sup>2</sup>; (n) VE55, 20 mJ/cm<sup>2</sup>; (o) VE55, 25 mJ/cm<sup>2</sup>; (p) VE55, 35 mJ/cm<sup>2</sup>.

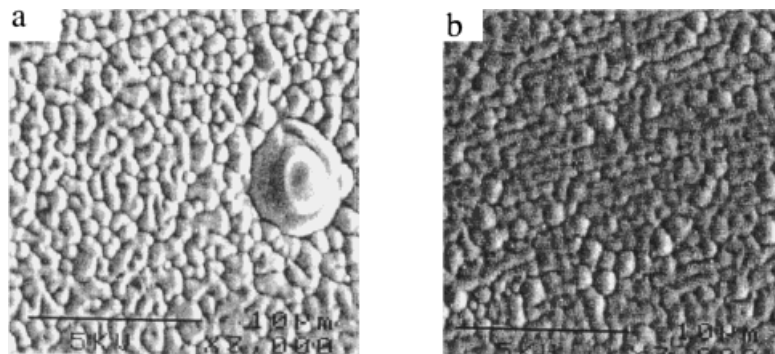


**Figure 6** SEM observation of vinylester material with 45 wt % styrene (VE45 sample) and unsaturated polyester G710 material with 45 wt % styrene (B45 sample) after ArF laser excimer treatment (193 nm radiation) with  $25 \text{ mJ/cm}^2$ . Magnification is  $3000\times$ .

hydrogen bonding. The polymer microparticles were formed within the early stage of polymerization process and were very swellable and present a very well organized morphology. The synthesis of this microgel species followed the typical dispersion polymerization process.

This VE structure arrangement is an additional element that could explain the very good hydrolysis stability of these materials with respect to unsaturated polyesters; the chemical stability of the ester functions in the presence of water does not make it possible to fully explain the polyester type materials. The fact that the materials are structured could limit the differences in pressure between the various phases and improve the overall stability of the vinylesters in a humid environment.

## CONCLUSION

A technique based on the use of an ArF excimer laser (193 nm) to analyze the morphology of the unsaturated polyester and vinylester networks has been developed. This method is based on the use of the differences between the thresholds at which ablation of the various constituent phases of the materials occur.

The threshold at which ablation of a polystyrene crosslinked by a radical mechanism occurs was determined at  $15 \text{ mJ/cm}^2$ , whereas the ablation thresholds for the polyester phases observed in the UP materials were determined as between 25 and  $35 \text{ mJ/cm}^2$ . With the VEs, the threshold is  $25 \pm 2 \text{ mJ/cm}^2$ . A surface treatment was applied to vinylester type materials with energy intensities in the vicinity of these thresholds. A two-

phase structure comprising microgels in a polystyrene phase was shown by SEM observation, making it possible to conclude that the mechanisms by which the unsaturated polyester and vinylester networks are formed by microgelling are similar. These observations confirm the findings made by IR observations of the polymerization kinetics previously conducted, and which concluded in cross-linking by formation of a phase rich in vinylester networking (microgels), which was included at the end of the process in a polystyrene matrix.

In addition, as concerns the morphology of the VE materials, we observed that the two-phase structure of the vinylester matrices, unlike that of the unsaturated polyesters, was organized in a random-oriented way, which could represent an important parameter contributing to the very good hydrolysis stability of these materials. In the event of degradation by osmotic mechanisms, the organized structure network would enable limiting the development of the osmotic pressures by distributing the forces within the material, thus avoiding crazing.

The Cray Valley/Groupe Total Society, who gave us the unsaturated prepolymer polyester, is gratefully acknowledged.

## REFERENCES

1. I. H. Updegraff, in *Handbook of Composites*, G. Lubin, Ed., Van Nostrand Reinhold, 1982, pp. 19–37.
2. K. Horrie, I. Mita, and H. Kambe, *J. Polym. Sci.*, **A1**, 2839 (1970).

3. K. Horrie, I. Mita, and H. Kambe, *J. Polym. Sci.*, **A1**, 2561 (1969).
4. Y. S. Yang and L. J. Lee, *Polym. Process. Eng.*, **5**, 327 (1987).
5. Y. S. Yang, and L. J. Lee, *Macromolecules*, **20**, 1490 (1987).
6. Y. S. Yang, and L. J. Lee, *Polymer*, **19**, 1793 (1988).
7. Y. S. Yang, L. Suspène, *Polym. Eng. Sci.*, **31**, 321 (1991).
8. L. Suspène, E. Pezron, and Y. S. Yang, paper presented at the 47th Annual Conference of the Composite Institute, SPI, Session 13A, 1992.
9. M. S. Lin, R. J. Chang, T. Yang, and Y. F. Shin, *J. Appl. Polym. Sci.*, **55**, 1607 (1995).
10. Y. J. Huang and C. C. Su, *Polymer*, **35**, 2397 (1994).
11. S. Crump, 41st Annual Conference, SPI, Session 13C, Jan. 27–31, 1986.
12. P. Castaing, L. Lemoine, and A. Gourdenne, *Comp. Struct.*, **30**, 217 (1995).
13. P. Castaing, L. Lemoine, and A. Gourdenne, *Comp. Struct.*, **30**, 223 (1995).
14. K. H. G. Ashbee, F. C. Franck, and R. C. Wyatt, *Proc. Roy. Soc.*, **A300**, 495 (1967).
15. H. P. Abeysinghe, W. Edwards, G. Pritchard, and G. J. Swanpillai, *Polymer*, **23**, 1785 (1982).
16. R. C. Adams, 37th Annual Conference on Reinforced Plastics, SPI, Session 21B, Jan. 11–15, 1982.
17. B. Mortaigne, V. Bellenger, and J. Verdu, *Polym. Network Blends*, **2**, 187 (1992).
18. M. Ganem, B. Mortaigne, V. Bellenger, and J. Verdu, *Polym. Network Blends*, **4**, 87 (1994).
19. M. Ganem, B. Mortaigne, V. Bellenger, and J. Verdu, *Polym. Network Blends*, **4**, 115 (1994).
20. M. Ganem, B. Mortaigne, V. Bellenger, and J. Verdu, *J. Macromol. Sci., Pure Appl. Chem.*, **A30**, 829 (1993).
21. K. Kato, *J. Electron Microsc.*, **14**, 220 (1965).
23. J. W. Dini, *SAMPE J.*, **32**, 58 (1996).
22. J. J. Hebert, T. P. Hensarling, T. J. Jacks, and R. J. Berni, *J. Appl. Polym. Sci.*, **23**, 2929 (1979).
24. T. R. Jervis, *J. Adv. Mater.*, **25**, 4 (1993).
25. R. Srinavan, *J. Appl. Phys.*, **73**, 2743 (1993).
26. S. Lazare and V. Granier, *Laser Chem.*, **10**, 25 (1989).
27. S. R. Cain, F. C. Burns, and C. E. Otis, *J. Appl. Phys.*, **71**, 4107 (1992).
28. A. Buchman, H. Dodiuk, M. Rotal, and J. Zahavi, *J. Adh. Sci. Technol.*, **8**, 1211 (1994).
29. B. Sadras, P. Laurens, F. Décobert, and F. Arefi, in *Proceedings of High Power Lasers: Applications and Emerging Applications*, Besançon, France, SPIE Series, Vol. 2789, 1996, p. 305.
30. A. Costela, J. M. Figuera, and F. Florino, *Appl. Phys.*, **60**, 261 (1995).
31. G. C. D' Couto, S. V. Babu, F. D. Egitto, and C. R. Davis, *J. Appl. Phys.*, **74**, 5972 (1993).
32. D. Singleton, G. Paraskevopoulos, and R. Taylor, *Chem. Phys.*, **114**, 415 (1990).
33. J. F. Rudd, in *Polymer Handbook*, 3rd ed., J. Brandup and E. H. Immergut, Eds., Wiley, New York, 1989.
34. D. Saatweber, and B. Vogt-Birnbrich, *Prog. Org. Coat.*, **28**, 33 (1996).
35. K. E. J. Barrett, *Dispersion Polymerization in Organic Media*, Wiley, London, 1975.